Comparing paleo reconstructions of warm and cool season streamflow (1400–2018) for the North and South Saskatchewan River sub-basins, Western Canada

Samantha A. Kerr, Yuliya Andreichuk & David Sauchyn

◨ View supplementary material ⧉

▦ Published online: 15 Dec 2022.

✎ Submit your article to this journal ⧉

▥ Article views: 51

◹ View related articles ⧉

⬚ View Crossmark data ⧉

Taylor & Francis
Taylor & Francis Group

Check for updates

Comparing paleo reconstructions of warm and cool season streamflow (1400–2018) for the North and South Saskatchewan River sub-basins, Western Canada

Samantha A. Kerr[a], Yuliya Andreichuk[b] and David Sauchyn[a,b]

[a]Department of Geography and Environmental Studies, University of Regina, Regina, Canada; [b]Prairie Adaptation Research Collaborative (PARC), University of Regina, Regina, Canada

ABSTRACT

The North and South Saskatchewan River sub-basins comprise the Saskatchewan River Basin (SRB), which originates in the eastern slopes of the Rocky Mountains of Alberta (Canada) and Montana (USA), extending across the vast landscape of three Canadian Provinces. The SRB is the most populated region of the Northern Great Plains, where water demands from agriculture, industry, and municipalities can be a substantial proportion of supply during periods of low flow and hydrological drought. Changing climatic conditions and shifts between periods of extreme wet and dry weather emphasize the need for a better understanding of past and future seasonal variability of the surface water balance within and between the sub-basins. Climate extremes, such as hydrological drought and excessive moisture conditions occurring simultaneously can create detrimental effects. Using a multi-species network of over 80 tree-ring chronologies, warm (May through August) and cool (December through April) season streamflow (1400–2018) were independently reconstructed for the North and South Saskatchewan River sub-basins. Departures from seasonal flow and spectral and wavelet analyses of the reconstructions indicate significant variability at inter-annual and multi-decadal scales.

RÉSUMÉ

Les sous-bassins des rivières Saskatchewan Nord et Sud forment le bassin de la rivière Saskatchewan (BRS), qui prend sa source sur les pentes orientales des montagnes Rocheuses de l'Alberta (Canada) et du Montana (États-Unis) et s'étend sur le vaste territoire de trois provinces canadiennes. Le SRB est la région la plus peuplée des Grandes Plaines du Nord, où les demandes en eau de l'agriculture, de l'industrie et des municipalités peuvent représenter une proportion substantielle de l'approvisionnement pendant les périodes de faible débit et de sécheresse hydrologique. L'évolution des conditions climatiques et les changements entre les périodes de temps extrêmement humide et sec soulignent la nécessité de mieux comprendre la variabilité saisonnière passée et future du bilan des eaux de surface dans et entre les sous-bassins. Les extrêmes climatiques, tels que la sécheresse hydrologique et les conditions d'humidité excessive se produisant simultanément, peuvent avoir des effets néfastes. En utilisant un réseau multi-espèces de plus de 80 chronologies d'anneaux d'arbres, les débits de saison chaude (mai à août) et de saison fraîche (décembre à avril) (1400-2018) ont été reconstruits indépendamment pour les sous-bassins de la rivière Saskatchewan Nord et Sud. Les écarts par rapport au débit saisonnier et les analyses spectrales et par ondelettes des reconstruits indiquent une variabilité importante aux échelles interannuelle et multidécennale.

Introduction

The North Saskatchewan River (NSR) and South Saskatchewan River (SSR) sub-basins comprise the Saskatchewan River Basin (SRB). The SRB originates in the eastern slopes of the Rocky Mountains of Alberta (Canada) and Montana (USA), and extends across the heavily populated region of the Canadian Prairie Provinces (Figure 1). Annual hydrographs (not shown) for both rivers reflect mid-latitude, mountainous, snow-dominated watersheds. Approximately 50% of the mean annual stream discharge occurs in the summer months of June and July, when melt water from high elevation snowpack is the primary source of runoff, and high flows are maintained throughout

Figure 1. Study Area: North and South Saskatchewan River sub-basins, Saskatchewan, Canada.

August. Nival processes are key within the SRB, as winter snowpack is the primary source of summer water supply throughout the region, and spring and summer precipitation, as well as glacial mass wasting also contribute varying amounts (Pomeroy, de Boer, and Martz 2005; Comeau, Pietroniro, and Demuth 2009; Marshall et al. 2011; Kienzle et al. 2012; MacDonald et al. 2012). Annu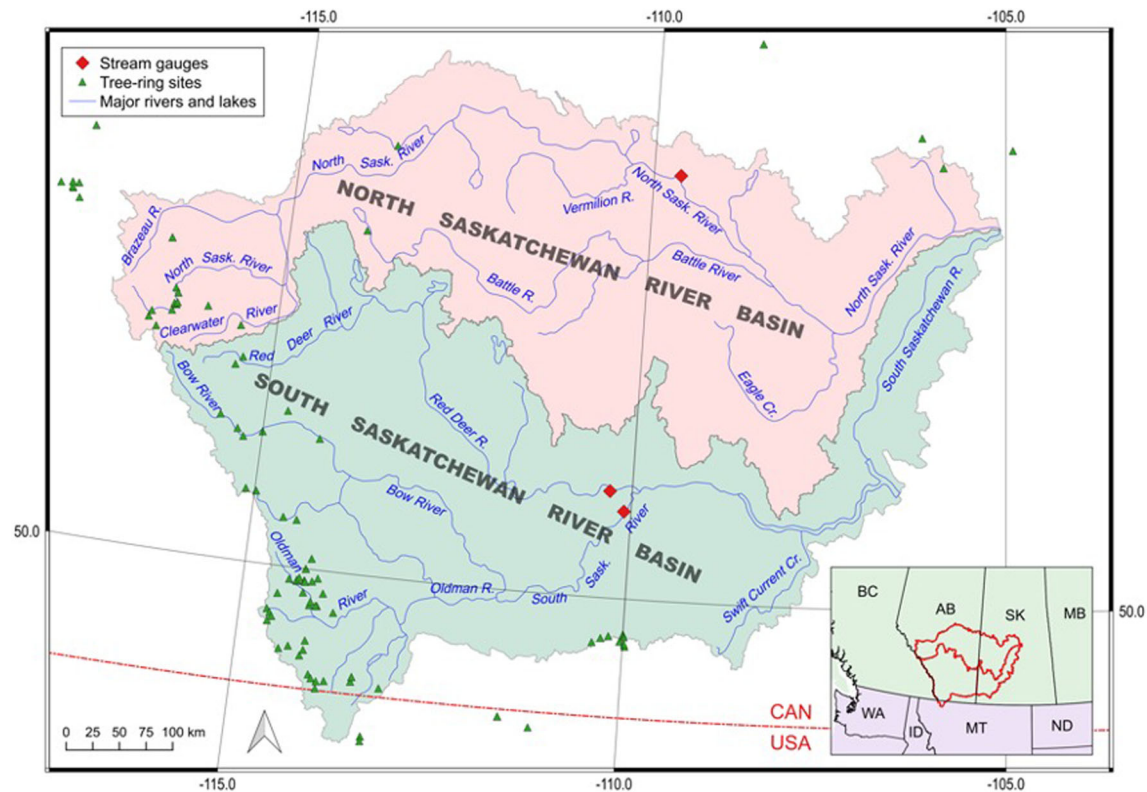al cycles of warm and cool season precipitation that define the hydrological regime of this region, are further influenced by climate oscillations originating in the Pacific Ocean, such as the Pacific Decadal Oscillation (PDO) and the El Niño Southern Oscillation (ENSO) (Bonsal, Shabbar, and Higuchi 2001; Shabbar and Skinner 2004; Gobena and Gan 2006; Bonsal and Shabbar 2008, 2011; Whitfield et al. 2010; St. Jacques, Sauchyn, and Zhao 2010, 2014; Lapp et al. 2013; Gurrapu et al. 2016; Gurrapu et al. 2021).

Changes in the spatial distribution of water resources on a seasonal and annual basis, as well as between watersheds, will be a major potential risk from changing climate in the Canadian Prairie Provinces, with the most challenging future scenario representing a shift in the frequency and severity of climate extremes and departures from average conditions (Sauchyn and Kulshreshtha 2008; Kulshreshtha, Nagy, and Bogdan 2012a, 2012b; Sauchyn et al. 2012; Bonsal et al. 2019).

Changes in the variability and trends in precipitation, winter temperature, glacial mass wasting, and mountain snowpack create uncertainty for downstream communities, which are reliant upon snowpack meltwater during the spring and summer months (Mote et al. 2018). Models project warmer winter temperatures, increased rainfall, and reduced snowpack under future climate change, which will alter the flow regime and timing of the regional annual and seasonal hydrograph characteristics of the NSR and SSR sub-basins (Rood et al. 2005; St. Jacques, Sauchyn, and Zhao 2010, 2014, 2018).

While the NSR and SSR sub-basins are adjacent (Figure 1) and hydrologically similar, throughout the sub-basins there are a variety of land uses and natural regions influencing the river systems differently. Rising population and economic activity have increased the demand for water supply, and therefore the region's vulnerability to extreme hydroclimatic events (Sauchyn et al. 2015). The use and demand for water differs throughout each sub-basin and also by province (North Saskatchewan Watershed Alliance 2007; Government of Alberta 2010; Kulshreshtha, Nagy, and Bogdan 2012a, 2012b; Thompson 2016). Rural and urban settlement, as well as agriculture, forestry, industry, and hydroelectric generation are dependent upon the runoff from the Rocky

Mountains. In Alberta, agricultural irrigation accounts for most of the consumptive use from the SSR, whereas agricultural, industrial and mining activities account for most of the consumptive use from the SSR in Saskatchewan (Kulshreshtha et al. 2012b). Industrial and municipal activity account for most of the consumptive use from the NSR in Alberta and Saskatchewan (North Saskatchewan Watershed Alliance 2007; Government of Alberta 2010; Kulshreshtha, Nagy, and Bogdan 2012a; Thompson 2016). Future recurrence and increased variability of climatic extremes, such as drought, will further impact the stress on regional water resources, agriculture, industry, aquatic ecosystems, and health (Asong et al. 2018).

A comprehensive understanding of the long-term spatial and temporal variability of seasonal water supply for the SRB is important to determine how the regional hydroclimate has varied in the past. We aim to provide insights for water resource managers to improve current design, management, risk assessment, and policies to address both natural hydroclimatic variability, and the impacts of future climatic change. Current management of infrastructure for the storage, allocation, and delivery of water is based on the analysis of instrumented weather and hydrological records, which are limited in length. Instrumental records, which range from 80 to 100 years throughout the Canadian Prairie Provinces, underestimate the potential worst-case scenarios for drought conditions, and provide limited perspective on the relationship of the regional hydroclimate to low-, mid- and high- frequency ocean-atmospheric oscillations over the long-term (Torbenson 2019).

Inter- and intra-annual and multi-year climatic extremes create uncertainty about the sustainability of water resources for municipal, industrial, and agricultural purposes. Understanding the long-term internal natural variability of the regional hydroclimate of the SRB, is an important precursor to research on the impacts and effects of climate change. Natural proxy records of hydroclimatic behaviour, such as tree-ring chronologies, provide a depth of knowledge of the past at both fine spatial and temporal resolutions.

Tree-ring chronologies provide exactly dated and hydro-climatically sensitive proxy data that can represent a large geographic area. Throughout the low- to mid- elevations of the headwaters of the SRB, on the eastern slopes of the Rocky Mountains, there are long-lived moisture sensitive coniferous trees including limber pine (*Pinus flexilis*), ponderosa pine (*Pinus ponderosa*), lodgepole pine (*Pinus contorta*), whitebark pine (*Pinus albicaulis*), tamarack (*Larix laricina*), and Douglas-fir (*Pseudotsuga menziesii*) species. Tree-ring data from long-lived trees growing at moisture sensitive sites may operate as a proxy for seasonal and annual water levels. When this is the case, tree growth is limited by available soil moisture and thus the same weather variables (precipitation, temperature, and evapotranspiration) that determine streamflow. There is also a similar integrating and lagged response of tree growth and streamflow to precipitation and evapotranspiration (Sauchyn and Ilich 2017), and therefore stream discharge tends to be significantly correlated with ring-width chronologies from moisture sensitive trees.

Tree-ring data have been used for dendrohydrological reconstructions of streamflow, at inter-annual to multi-decadal timescales, in most of the river basins in Canada's western interior, including the SSR (Axelson, Sauchyn, and Barichivich 2009) and NSR (Case and MacDonald 2003; Sauchyn, Vanstone, and Perez-Valdivia 2011, Sauchyn et al. 201b; Sauchyn and Ilich 2017). Some of these reconstructions have been applied to water supply models in water resource management with the City of Calgary and Edmonton Power Corporation (EPCOR) (Sauchyn, Vanstone, and Perez-Valdivia 2011, Sauchyn et al. 2015; Sauchyn and Ilich 2017). More recent dendroclimatic studies throughout western Canada and North America, have employed networks of tree-ring chronologies and sub-annual earlywood (EW) and latewood (LW) width to estimate seasonal scale changes in the regional hydroclimate (Watson and Luckman 2006; Starheim, Smith, and Prowse 2013; St. George 2014; Coulthard and Smith 2016; Crawford, Griffin, and Kipfmueller 2015; Coulthard, Smith, and Meko 2016; Dannenberg and Wise 2016; Howard, Stahle, and Feng 2019; Lopez et al. 2019; Torbenson 2019; Welsh, Smith, and Coulthard 2019; Coulthard et al. 2021; Mood, Coulthard, and Smith 2020; Stahle et al. 2020; Wise 2021; Kerr, Andreichuk, and Sauchyn 2021). Other dendroclimatological studies have also assessed the importance of glacial mass balance and the implications of modern hydrometric data (Watson and Luckman 2006; Coulthard and Smith 2016; Welsh, Smith, and Coulthard 2019; Coulthard et al. 2021; Mood, Coulthard, and Smith 2020; Anis et al. 2021).

Analysis of separate tree-ring reconstructions of warm (May through August) and cool (December through April) season streamflow is possible because tree-ring data from different sites within and adjacent to the study area are sensitive to the cold and warm

seasonal moisture balance (Torbenson et al. 2016; Torbenson 2019; Stahle et al. 2020; Wise 2021; Kerr, Andreichuk, and Sauchyn 2021), providing a large spatial scale assessment of the regional hydroclimate (Kerr, Andreichuk, and Sauchyn 2021). For this analysis, the warm season period includes the greatest melt of mountain snowpack and glaciers, precipitation, and the growing season. The cool season concludes with snowmelt and the recharging of soil moisture prior to the growing season. While the warm and cool season time periods used within this analysis do not coincide to the typical studies of standard meteorological seasons, we aim to highlight the importance of the timing and spatial extent of the regional hydroclimate (Wise 2021; Kerr, Andreichuk, and Sauchyn 2021). Hydroclimatic conditions prior (i.e. the cool season) to and during the warm season are especially significant for water quality and quantity for agriculture, municipalities, and industry. These palaeohydrological reconstructions provide context for better understanding of the long-term seasonal and spatial characteristics of the pre-instrumental hydroclimate of the SRB, and the ability to determine when both sub-basins have been impacted by sustained droughts or excess moisture events simultaneously.

The objective of this research is to provide water management agencies in the Canadian Prairie Provinces, with robust seasonal palaeohydrological reconstructions of streamflow. Water delivery, allocation, storage, and treatment infrastructure and protocols under extreme hydroclimatic conditions, can be assessed through the development of seasonal tree-ring reconstructed streamflow for the NSR and SSR sub-basins of the SRB. We analyse the reconstructed seasonal streamflow in terms of the frequency and magnitude of flows, and compare seasonal anomalies of wet and dry periods between sub-basins of the SRB. Further, we analyse the potential relationships between hydroclimate-related variables and the long-term influence of commonly cited periodicities of high to middle frequency climate oscillations on that variability (Ault et al. 2013; Sauchyn and Ilich 2017; Bonsal et al. 2019).

Data and methodology

Tree-ring chronologies

We use a network of over 80 multi-species tree-ring chronologies, which were developed in the University of Regina Tree-ring Laboratory, from the headwaters of the SRB and adjacent river basins. This extensive multi-species tree-ring network provides the potential to better capture the seasonal and spatial hydroclimatic variability of the SRB, better reflecting the seasonal or intra-annual contribution of moisture surpluses and deficits (Meko and Baisan 2001; Griffin et al. 2013; St. George 2014; Torbenson et al. 2016; Sauchyn and Ilich 2017; Lopez et al. 2019; Stahle et al. 2020; Kerr, Andreichuk, and Sauchyn 2021).

Sampling and chronology preparation, as well as cross-dating the tree-ring chronologies, followed standard dendrochronological procedures (Stokes and Smiley 1968; Fritts 1976, Cook et al. 1990). A full description of the methodology used for building the tree-ring chronologies can be found in Sauchyn, Vanstone, and Perez-Valdivia 2011. A minimum of 20–30 trees and two samples/tree were obtained at each chronology location. Samples collected from both living (cores) and dead (disks) trees were sanded with progressively finer sand paper to make distinct annual (RW-), EW-, and LW- growth rings clearly visible. Within conifer species, there are two distinct layers visible within the annual ring, which are directly related to seasonal changes in light, temperature, and moisture (Fritts 1976). EW, which is produced early in the growing season when soil moisture is abundant or least sufficient, is composed of low-density light-coloured cells, while LW, which is produced later in the growing season, when growth becomes moisture and/or temperature limited, has smaller darker cells which have thicker walls (Fritts 1976). The development of these separate measurements and chronologies often provides greater sub-annual information on the influence of the regional hydroclimate (St. George 2014; Torbenson et al. 2016; Sauchyn and Ilich 2017; Howard, Stahle, and Feng 2019; Lopez et al. 2019; Torbenson 2019; Welsh, Smith, and Coulthard 2019; Coulthard et al. 2021; Stahle et al. 2020; Wise 2021; Kerr, Andreichuk, and Sauchyn 2021).

RW-, EW-, and LW- width were measured from high-resolution scanned images, with precision of 0.001 mm, and manually cross-dated using the software package WinDendro Density 2019 (Regent Instruments Inc. 2019), a semi-automated image analysis system. To validate the manual cross-dating from the high-resolution images of tree-ring widths, the statistical program COFECHA (Holmes 1983), which uses segmented cross-correlation techniques for detection of measurement and manual cross-dating errors, was used to assign the exact calendar year to each ring. The expressed population signal (EPS) of at least 0.85 (Wigley, Briffa, and Jones 1984) was used to determine whether the sample size was adequate.

Table 1. Properties of tree-ring chronologies that comprise the pool of potential predictors.

Site Code	Latitude	Longitude	Elevation (m. asl)	Species	# Trees	Years
BBC	48.2	−109.5	1403	PIPO	8	1572–2002
BBR	48.2	−109.6	1403	PIPO	12	1668–2002
BCK	49.8	−113.9	1592	PSME	16	1601–2006
BCR	48.1	−109.6	1245	PIPO	30	1723–2010
BCT	51.1	−115.3	1405	PSME	19	1548–2013
BCW	49.9	−114.2	1686	PSME	19	1579–2004
BDC	49.9	−114.2	1661	PSME	22	1504–2005
BMN	49.9	−114.0	1297	PIFL	20	1254–2007
BND	49.0	−113.9	1297	PSME	21	1758–2005
BOB	49.9	−114.3	1450	PSME	29	1525–2012
BOY	48.1	−109.6	1245	PSME	31	1580–2010
BPM	48.2	−109.7	1800	PSME	12	1621–2002
BRR	49.7	−114.1	1320	PSME	8	1768–2004
BSG	52.6	−116.6	1810	PCGL	35	1669–2003
BTC	50.0	−114.2	1536	PSME	32	1595–2015
BVL	49.4	−114.1	1427	PSME	32	1651–2004
BZR	49.1	−113.5	1468	PIFL	42	1467–2007
CAB	49.7	−114.0	1395	PSME	36	1354–2016
CAL	50.0	−114.2	1677	PSME	20	1613–2004
CBR	48.6	−113.3	1673	PIFL	25	1312–2006
CFM	49.1	−113.8	1500	PSME	16	1802–2005
CHP	49.7	−110.0	1000	PICO	27	1860–2001
CMT	49.1	−113.9	1284	PSME	8	1857–2002
CNL	49.6	−114.6	1384	PIFL	20	1579–2007
CPH	49.6	−110.0	1334	PCGL	88	1843–1997
DCK	49.9	−114.4	1648	PSME	42	1619–2004
DEA	52.2	−116.4	1320	PSME	37	1471–2018
DMH	52.9	−118.1	1040	PSME	16	1677–2013
GRF	52.9	−113.9	1720	PICO	35	1528–2006
GRN	53.6	−113.7	655	PCGL	23	1868–2011
HEM	49.7	−113.8	1308	PIFL	48	1326–2015
HIP	50.6	−114.9	2200	LALA	28	1470–2016
HWM	47.5	−110.6	1580	PSME	28	1648–2006
JOL	51.9	−115.5	1405	PSME	30	1380–2016
LBC	49.9	−114.2	1602	PSME	23	1521–2004
LBM	46.9	−110.9	1830	PSME	8	1699–2005
LEC	49.1	−113.5	1258	PSME	22	1738–2009
LEE	49.1	−113.5	1258	PIFL	10	1579–2009
MDP	47.2	−109.2	1666	PSME	12	1525–2003
MGC	52.9	−118.0	1200	PSME	19	1757–2018
MVP	49.6	−110.4	1350	PCGL	16	1870–2009
NQY	51.2	−115.6	1650	PSME	36	1590–2013
OCC	49.7	−114.1	1280	PICO	15	1684–2003
OCG	52.1	−115.9	1940	PCGL	18	1669–2003
OMM	49.9	−114.2	1331	PSME	54	1491–2016
OMR	49.8	−114.2	1427	PIFL	95	933–2015
PEC	50.4	−114.4	1515	PIFL	29	1667–2005
PLK	52.8	−118.1	1130	PSME	23	1725–2018
PNR	51.6	−115.5	1790	PIFL	16	1577–2012
PRB	49.3	−114.1	2093	PIAB	18	1706–2011
RIC	49.9	−114.2	1667	PIFL	16	1708–2002
SBL	51.9	−116.7	2051	PIAB	32	1511–2007
SCT	47.6	−108.5	802	PIPO	34	1662–2003
SFR	52.0	−116.4	1390	PIFL	39	542–2018
SGH	48.9	−111.5	1700	PSME	34	1338–1996
SIP	51.1	−115.0	1597	PSME	16	1600–2003
SKC	51.9	−116.7	1423	PIFL	33	1109–2007
SPC	49.7	−110.2	1309	PICO	19	1881–2009
STR	51.1	−114.2	1095	PSME	11	1575–2013
SWB	54.8	−115.6	1733	PIBA	17	1734–2004
SWG	54.7	−115.6	1752	PCGL	5	1753–2004
TAB	49.3	−114.4	1838	LALA	32	1616–2010
TTB	52.9	−118.1	1310	PSME	30	1652–2019
TWO	52.1	−116.4	1560	PSME	33	1481–2018
UPL	50.6	−115.1	1725	PCEG	22	1450–2012
VIC	49.8	−114.5	1909	PIAB	27	1233–2010
VIR	49.3	−114.2	2102	PIAB	19	1727–2011
VRL	52.9	−118.3	1210	PSME	18	1660–2013
WBS	48.9	−111.5	1904	PIAB	33	1691–2010

(continued)

Table 1. Continued.

Site Code	Latitude	Longitude	Elevation (m. asl)	Species	# Trees	Years
WBT	48.9	−111.5	1588	PSME	38	1552–2010
WCH	51.3	−114.7	1351	PSME	58	1213–2016
WCK	50.1	−114.1	1536	PSME	34	1691–2005
WDR	49.9	−114.2	1565	PSME	34	1425–2013
WIP	52.2	−116.4	1315	PIFL	29	1445–2018
WPP	52.0	−116.5	1356	PIFL	45	887–2018
WRC	52.1	−116.4	1420	PSME	30	1498–2018
WSC	49.9	−114.1	1575	PSME	41	1446–2016
WSL	49.3	−114.3	2060	PIAB	29	1372–2009
WSS	52.8	−117.9	1599	PSME	50	1598–2018
YAT	51.7	−115.4	1529	PIFL	4	1519–2002
ZTM	47.9	−108.5	1360	PIPO	30	1545–2003

Properties of the tree-ring chronologies are provided in Table 1.

Because ring width depends to some extent on the size (diameter) and age of a tree, the annual and intra-annual ring-width data were standardized using the program ARSTAN (Cook 1985). A negative exponential curve was applied to remove juvenile growth trends from the ring-width series. A cubic smoothing spline (with a 50% frequency response cutoff at a wavelength of 67% of the series length) was used for the series that could not be standardized using a conservative technique (Cook et al. 1990, 1999). Standardized ring-width time series were averaged for each tree-ring site, using a mean value function that minimizes the effects of outliers (Cook et al. 1990), producing a dimensionless stationary index with a defined mean of 1.0 and a relatively constant variance. Chronology statistics (Cook and Kairiukstis 1990) for each standardized chronology are provided in the supplemental information (Table S1). Chronology length ranges from 300 to ≥ 1000 years (Table S1), and significant ($p < 0.05$) series inter-correlation and high mean sensitivity (> 0.3) indicate a strong common response to inter-annual variability in the hydroclimate. The length of each chronology was limited to the segment with an EPS ≥ 0.85, minimizing the inflation of variance associated with decreasing sample size (Wigley, Briffa, and Jones 1984; Table S1). This multi-species network of RW, EW, and LW chronologies were the pool of predictors for statistical models of naturalized warm and cool seasonal streamflow for the SRB.

Climate and streamflow data

To reconstruct the seasonal hydroclimate of the SRB, precipitation, temperature, and naturalized streamflow were compared to the network of standardized RW, EW, and LW chronologies using Pearson's correlation coefficient to summarize the strength of the

relationships between tree-rings and hydroclimatic variables. Gridded mean, maximum and minimum temperature (°C) and precipitation (mm) data, compiled by Natural Resources Canada (McKenney et al. 2011), were extracted for the SRB and converted into monthly, annual, and seasonal (warm (MAMJJA) and cool (DJFMA)) values. This 10-km interpolated gridded database provides complete uniform coverage throughout the SRB. Buffers of 50 to 500 km (in 50 km increments) were applied to determine which tree-ring sites could be used as predictors of hydroclimate (for each gridded station). Due to the random locations of tree-ring sites compared to the regular gridded climate data, it was determined that a buffer of 400 km would allow correlated hydroclimate variables to be included within the analysis. Further, thresholds of sample depth ($n \geq 20$) and age (≥ 50 years) were also considered, and then significant correlations of tree-ring sites and hydroclimatic variables were ranked ($p < 0.05$).

Alberta Environment and Parks provided naturalized daily and weekly streamflow data for the SSR (05AK001 at Highway 41) and NSR (05EF001 near Deer Creek) for the periods 1912–2009 and 1911–2010, respectively. These data were derived by the project depletion method, which uses streamflow records, reservoir data, recorded and estimated irrigation withdrawals, and adjusts the recorded flows to account for the effects of storage and diversions. A detailed description of this methodology is provided by Sauchyn and Ilich (2017). Naturalized streamflow was converted into monthly, annual, and seasonal (warm (MAMJJA) and cool (DJFMA)) averages. Warm and cool season streamflow were found to be normally distributed, according to a robust non-parametric Lilliefors test of normality ($p < 0.05$) (Lilliefors 1967) using a user-written MATLAB function. We calculated the mean, range, and standard deviation of the naturalized streamflow records to test the hypothesis that each record comes from a random sample of normal distributions. The Lilliefors statistic (Lilliefors 1967) indicated that the naturalized streamflow records are below critical threshold levels for rejecting the null hypothesis that each chronology comes from a normal distribution with unspecified mean and variance.

To examine whether tree-ring data were suitable predictors of streamflow in the NSR and SSR sub-basins, and to further investigate the seasonal response of tree growth to the hydroclimate in the SRB, standardized ring-width chronologies were then examined for their correlation (using Pearson's correlation; one tailed; $p < 0.05$) to monthly hydroclimate data for the grid point closest to the naturalized streamflow gauge location. Chronologies with the highest positive significant correlation to warm and cool season naturalized streamflow were deemed to be the pool of potential predictors for reconstructing the mean warm or cool season streamflow using multiple linear regression (MLR). To ensure that models were not overfit, the pool of predictors was formed from the most significant ($p < 0.05$) chronologies regarding their correlations with the predictands. All raw naturalized streamflow data are provided in the supplemental information (Tables S5–S8).

Tree-ring reconstructed streamflow

We reconstructed warm and cool season streamflow for the NSR and SSR from tree-ring measurements using standard dendrohydrology methodology (Meko, Woodhouse, and Morino 2012). As with all hydroclimatic reconstructions, the underlying climate proxies represent a source of uncertainty. In this case, uncertainty regarding the tree-ring chronologies was minimized by carefully selecting chronology sites, using multiple samples per tree, and ensuring sufficient replication (sample depth) for each chronology. In MATLAB, user-written MLR (function: regress) using a forward stepwise procedure with a cross-validation stopping rule, was used to model and reconstruct warm and cool season streamflow for 600 years for the NSR (near Deer Creek) and SSR (at Highway 41). Multiple species proxies of RW-, EW-, and LW-width were used as predictors of naturalized streamflow.

Nested reconstructions were developed to encompass more time, and thus, the varying tree-ring chronology lengths. In this procedure, we estimated streamflow from stepwise regression models for the time-period covering all individual chronologies, and then for progressively longer periods by successfully removing the shortest chronology from the pool of predictors. In our initial exploratory analysis, we identified time spans which corresponded to significant changes with declining sample depth. So, throughout the reconstruction, each subsequent nest encompasses more time, however, fewer tree-ring chronologies. This allowed the time coverage of the reconstruction to be maximized, as the reconstruction will extend to the earliest year of data for the oldest chronology. Predictors were entered stepwise until an additional predictor failed to increase the adjusted R^2. Each nested reconstruction joins the full reconstruction at the over-lap year. Therefore, each time-period is

Table 2. Chronologies used in nested palaeohydrological reconstructions for the SSR and NSR (see Table 1 for site codes, properties, chronology years).

Proxy Reconstruction			
SSR Cool Season Nest 1*	Nest 2	Nest 3	Nest 4
1400–2018 BMNRW(-1)	BMNRW(-1)	BMNRW(-1)	BMNRW(-1)
HEMLW(-1)	HEMLW(-1)	HEMLW(-1)	HEMLW(-1)
WDRLW(0)	WDRLW(0)	WDRLW(0)	
OMMLW(0)	OMMLW(0)	OMMLW(0)	
BCTRW(-2)	BCTRW(-2)		
LEELW(0)			
SSR Warm Season Nest 1	Nest 2	Nest 3	Nest 4
1400–2018 HEMRW(0)	HEMRW(0)	HEMRW(0)	HEMRW(0)
JOLLW(0)	JOLLW(0)	JOLLW(0)	CABLW(-1)
CABLW(-1)	CABLW(-1)	CABLW(-1)	
WSCEW(0)	WSCEW(0)		
BCTEW(-1)	BCTEW(-1)		
CNLLW(0)			
NSR Cool Season Nest 1	Nest 2	Nest 3	Nest 4
1400–2018 WPPLW(0)	WPPLW(0)	WPPLW(0)	WPPLW(0)
SKCLW(-1)	SKCLW(-1)	SKCLW(-1)	SKCLW(-1)
CBRLW(-2)	CBRLW(-2)	CBRLW(-2)	CBRLW(-2)
TWORW(0)	TWORW(0)	TWORW(0)	
BSGLW(0)	BSGLW(0)		
MGCLW(-2)			
NSR Warm Season Nest 1	Nest 2	Nest 3	Nest 4
1400–2018 SFRRW(0)	SFRRW(0)	SFRRW(0)	SFRRW(0)
WPPEW(0)	WPPEW(0)	WPPEW(0)	WPPEW(0)
SKCRW(0)	SKCRW(0)	SKCRW(0)	SKCRW(0)
DEALW(0)	DEALW(0)	DEALW(0)	
WRCLW(-1)	WRCLW(-1)		
PECRW(0)			

*RW = ring-width chronology; EW = earlywood chronology; LW = latewood chronology; 0 = no lag; -1 = negative 1-year lag; -2 = negative 2-year lag

represented by the corresponding regression model, with the maximum sample depth. Chronologies used within each nested reconstruction of warm and cool season streamflow for the SSR and NSR are provided in Table 2. Streamflow reconstructions of the SSR and NSR (1400–2018) are shown in Figure 2, as percent anomalies from mean values for warm and cool seasons.

Regression models were validated using a leave n-out method, where observations were left out sequentially throughout the length of the streamflow records. A series of regression models were fitted, and for each model deleting a different observation from the calibration set and using the model to predict the predictand for the deleted observation (Hughes et al. 1982). Throughout the calibration period of recorded streamflow, the strength of a regression model was expressed as the adjusted coefficient of multiple determination (R^2_{adj}). Further statistical tests (see below) were used to determine whether the distribution of errors satisfied the assumptions of a time series application of MLR, and results are presented below. Simulated warm and cool season streamflow for the SRB are provided in the supplemental information (Table S7).

To evaluate any similarities and differences in the timing, frequency, and magnitude of extreme hydroclimatic events between the sub-basins of the SRB, years of low flow (25th percentile), extreme hydrological drought (10th percentile), and high flows (75th percentile) were identified and compared for each season between both sub-basins.

We explored the reconstructed timeseries for the possible connections between hydroclimatic variables and the influence of large-scale ocean-atmosphere oscillations, driving the natural variability in the regional hydroclimate. Palaeohydrological records can be used to evaluate how hydroclimatic variables have changed over time and throughout positive (warm) and negative (cool) phases of climate oscillations. We identified the main modes of variability via the use of the multi-taper method (MTM; Mann and Lees 1996; Ghil et al. 2002) of singular spectral analyses and continuous wavelet analyses (CWT; Grinsted et al. 2004) to investigate any possible trends, spatial-temporal patterns, periodicities, and tele-connectivity of drought and excess moisture events. In MATLAB, user-written CWT was used to identify non-stationary signals as it decomposes the time series into frequency components. We used the Morlet wavelet with a wavelet power of significance tested at a 95% confidence level against a red-noise background. The MTM is a non-parametric method of spectral estimation widely used for atmospheric and oceanic variables, and does not describe an *a priori* model for the process generating the time series (Ghil et al. 2002). The MTM spectral analysis, using the SSA-MTM toolkit (Ghil et al. 2002), was performed on the warm and cool season reconstructions of streamflow to evaluate dominant frequencies of variability within the time series. The MTM uses orthogonal windows (tapers) to obtain independent estimates of the power spectrum and averages them to yield a more stable spectral estimate (Ghil et al. 2002). The MTM was used to determine high (highly variable from year to year) and low frequencies (gradual changes over decades or centuries) within the time series, while CWT, supplementing the MTM analyses, was used to investigate the temporal features of the time series. Extracted time series were compared to the PDO and ENSO indices.

Results

Tree-ring chronologies, climate and streamflow

For most chronologies (RW, EW, and LW), Pearson's correlation analysis indicated significant positive and
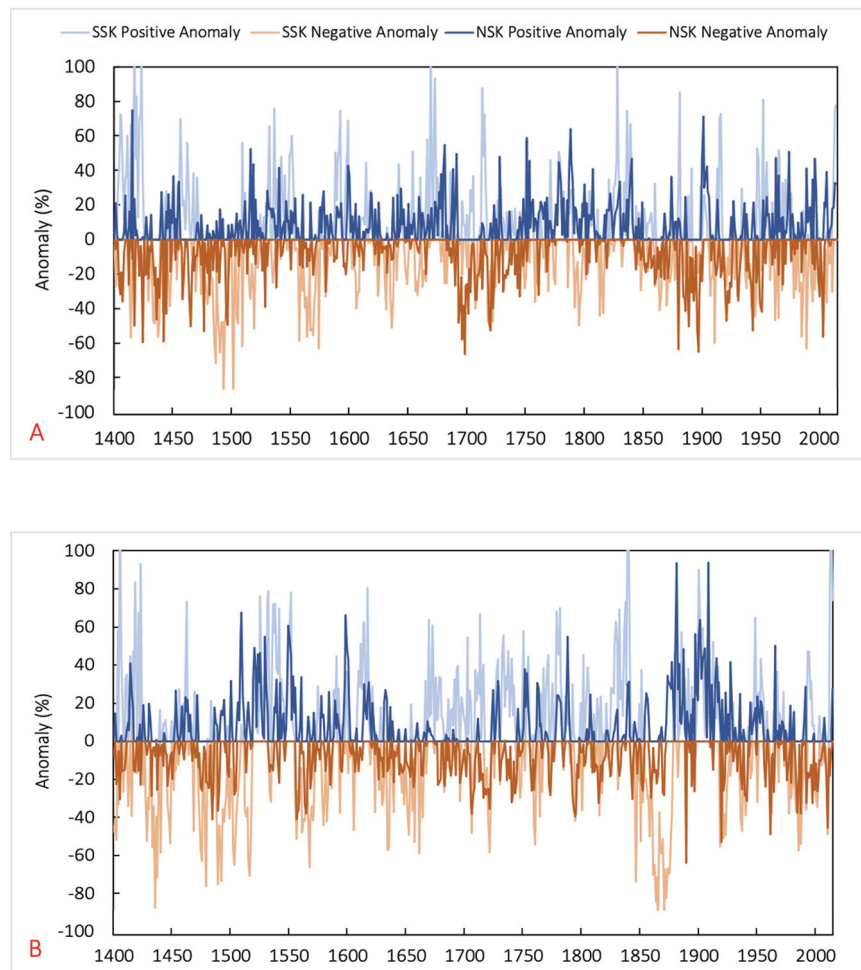
Figure 2. South Saskatchewan River (05AK001 at Highway 41) and North Saskatchewan River (05EF001 near Deer Creek) sub-basin cool (A) and warm (B) season reconstructed streamflow (shown as percent anomalies), 1400–2018.

negative correlation with mean seasonal and annual precipitation and temperature, respectively, and significant positive correlation with mean annual, seasonal, and water-year naturalized streamflow. This preliminary analysis revealed high significant positive correlation with both warm and cool season time periods (results not shown). The results of the correlation analysis indicated significant ($p < 0.05$) positive (negative) correlation of standardized index chronologies with mean seasonal and annual precipitation (temperature), for the current and previous years, suggesting that there is a moisture signal within the tree-rings. There were 120, 139, and 59 standardized chronologies that were significantly correlated ($p < 0.05$) with annual, warm season and cool season precipitation, respectively, for the grid point nearest 05AK001 at Highway 41 for the SSR. While for the NSR (05EF001 near Deer Creek), there were 89, 48, and 70 standardized chronologies that were significantly correlated ($p < 0.05$) with annual, warm season and cool season precipitation, respectively. Significant

($p < 0.05$) positive correlations (244 (SSR) and 77 (NSR) chronologies) were also found between standardized tree-ring chronologies and warm and cool season streamflow for the current and previous years (results not shown).

Paleohydrology of the SRB

Warm and cool seasonal hydrological records for the SSR (at Highway 41) and NSR (near Deer Creek) were extended back to 1400 AD, by nesting a series of reconstructions (Table 2 and Figure 2). The reconstructions replicated the inter-annual variability in historical streamflow, but are better at capturing low flows, while underestimating high flows, throughout the calibration period. Underestimation of peak flows is a common limitation of tree-ring reconstructions, as there is a biological limit to the response of tree growth to high precipitation and low evapotranspiration during wet years (Fritts 1976; Meko and Woodhouse 2011; Meko, Woodhouse, and Morino

Table 3. Calibration and verification statistics.

Proxy Reconstruction	Calibration and Verification Statistics						
	R^2	R^2_{adj}	SE	RE	$RMSE_v$	Portmanteau (Q)	Durbin Watson (DW)
SSR Cool Season	0.70	0.67	26.32	0.60	28.70	21.0	2.02
SSR Warm Season	0.74	0.71	97.72	0.68	101.72	25.1	2.33
NSR Cool Season	0.58	0.55	19.02	0.38	19.99	7.0	1.79
NSR Warm Season	0.57	0.54	85.12	0.50	87.93	9.5	2.20
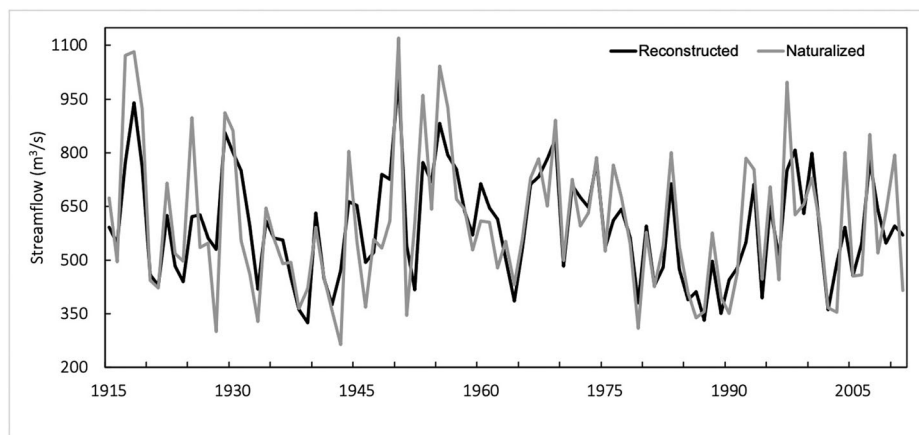
Figure 3. South Saskatchewan River (05AK001 at Highway 41) warm season instrumental and reconstructed streamflow (m3/s), 1913–2010.

2012). Calibration and verification statistics for the models indicate skilful reconstructions of warm and cool season streamflow (Table 3) from robust models with considerable predictive power. The models accounted for up to 71% of the naturalized streamflow instrumental variance (Figure 3). Time series plots of the regression residuals indicated relatively constant variance, and plots of the residuals against predicted values of the predictand and the individual predictors presented a lack of correlation. Histograms of the residual values showed an approximate normal distribution of errors (results not shown). Nested models were discarded prior to 1350, as R^2_{adj} values began to decline to below 35%, and other descriptive statistics indicated the model power was declining, due to a lack of sample depth.

The Durbin-Watson (DW) (Cook and Kairiukstis 1990; Draper and Smith 1998; Cook and Pederson 2011) statistic tests for autocorrelation of residuals, and values of the DW statistic supported a null hypothesis of no significant ($p = 0.05$) first order autocorrelation. The DW test for all models indicated no significant autocorrelation in the residuals during both calibration and validation periods. The Portmanteau (Q) statistic (Ostrom 1990) suggested that the residuals were not generated by an autoregressive or moving average model. For the verification period, we used the reduction of error (RE) statistic, a measure of association between a series of actual

values and their estimates. RE ranges from a maximum of +1, to negative infinity, and any positive value indicates that the model has some predictive capacity (Fritts 1976; Cook and Kairiukstis 1990). The F ratio of the regression model was computed as a goodness of fit statistic, and we also computed the standard error (SE) and the $RMSE_v$ (root-mean square error of validation), a measure of uncertainty in predicted values over the calibration and validation periods, respectively. SE and $RMSE_v$ have similar magnitude, suggesting accurate estimates of warm and cool season streamflow. A summary of the calibration and verification statistics is provided in Table 3.

The reconstructions of warm and cool season streamflow for the SRB reflect the natural variability of the tree-ring proxy records and the regional hydroclimate. The low flow years of the instrumental record (i.e. 1930s, 1980s, and early 2000s) are especially visible, where low flows are particularly extreme relative to the rest of the observed records. Even more noticeable are periods of low flow that exceed the historical worst-case scenario in terms of severity and duration (i.e. mid to late 1400s, Figure 2). The decadal scale variability is also evident within the figures provided below, in terms of successive years of high and low flows, which last one to three decades. The most notable dry periods occurred in the 1400s for both sub-basins for both warm and cool seasons, as well as the
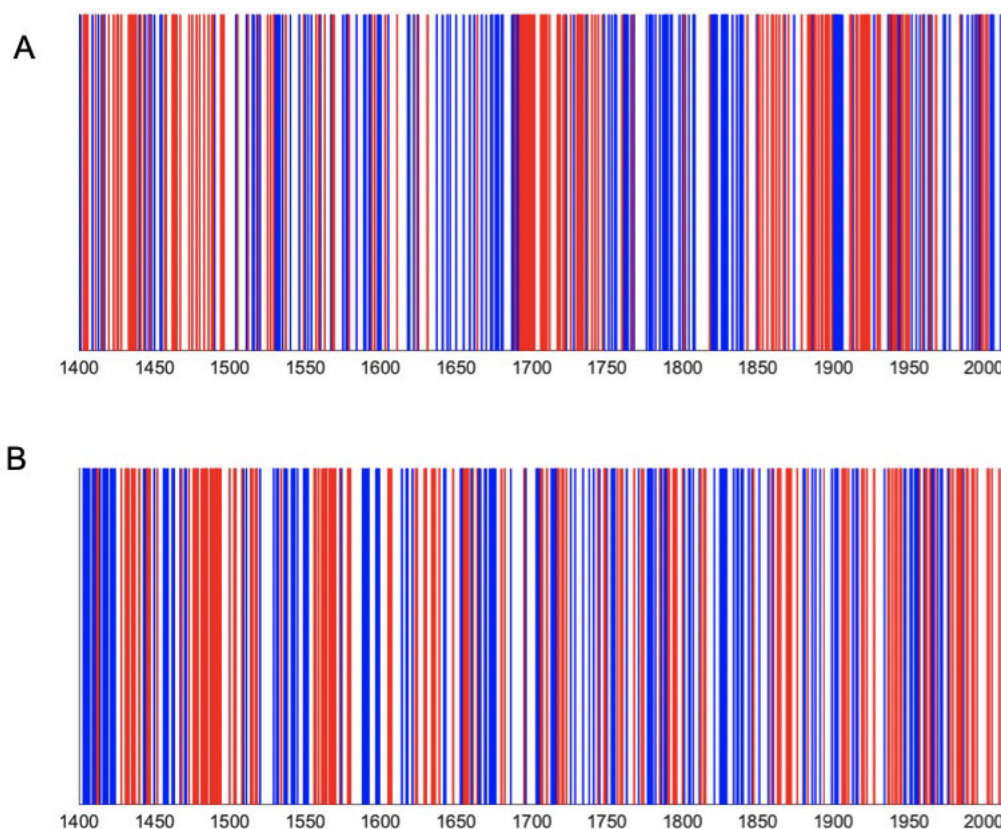
Figure 4. Reconstructed streamflow (1400–2018) for the SSR at Highway 41 (A) and the NSR near Deer Creek (B), defined on the 10th (in red) and 75th (in blue) percentile threshold of mean cool season streamflow.

late 1500s for warm seasons. Extensive dry periods throughout the 18th eighteenth century are also persistent throughout all streamflow reconstructions.

Figures 4 and 5 illustrate the pre-instrumental record of hydroclimatic variability by highlighting, for the warm and cool seasons, severe hydrological droughts, defined by the lowest 10th percentile, and years of excess moisture, defined by the 75th percentile. There are distinct differences between the sub-basins. The most sustained wet periods throughout the entire time series for the SSR (warm) was the mid-1500s and SSR (cool) was the 1400s and mid-1500s, while for the NSR (warm) was during the late-1400s, early-1500s, and late-1800s, and the late-1700s for the NSR (cool). The longest and most severe hydrological droughts occurred during the 1450s and 1850s for the SSR (warm) and the 1450s for the SSR (cool), while during the 1700s for the NSR (warm), and early-1400s, 1700s and late-1800s for the NSR (cool).

Evident dry and wet periods exist throughout the reconstructed time series, and the years of extreme hydroclimatic events indicate that there are more similarities between basins in both seasons during wet periods, than dry. It is also apparent that there are

more multi-year/basin events during the warm season for hydrological drought and low flow years, compared to years where excess streamflow occurred throughout the basins. Tables 4–6 summarize the same years of hydrological drought (defined by the 10th percentile), low flow years (defined by the 25th percentile), and years of excess moisture (defined by the 75th percentile) between the sub-basins, as well as the top 10 hydrological events in each season and sub-basin. For the cool season, there were 8, 43, and 51 similar years between the sub-basins defined by the 10th, 25th, and 75th percentiles, while for the warm season, there were 15, 60, and 54 similar years. All instances of hydrological drought, low-flow, and excess moisture throughout the reconstructions are provided in the supplemental information (Tables S2–S4).

Time series of naturalized warm and cool season streamflow for the SSR and NSR show inter-annual and decadal modes of variability (Figure 6), which have been commonly linked to the influence of ENSO and PDO on the hydroclimate of western North America (St. Jacques, Sauchyn, and Zhao 2010; Ault et al. 2013; Sauchyn et al. 2015, Gurrapu et al. 2016; Sauchyn and Ilich 2017; Gurrapu et al. 2021). Highly
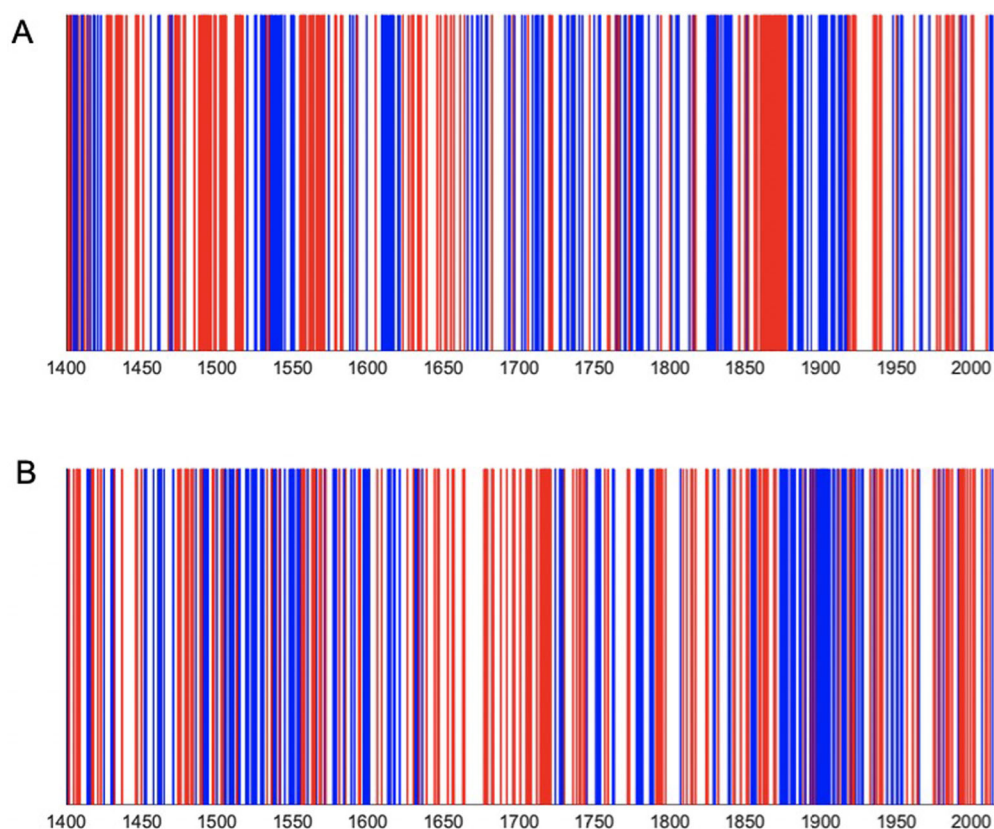
Figure 5. Reconstructed streamflow (1400–2018) for the SSR at Highway 41 (A) and the NSR near Deer Creek (B), defined on the 10th (in red) and 75th (in blue) percentile threshold of mean warm season streamflow.

Table 4. Same years of hydrological drought (defined by the 10th percentile) between sub-basins and the top 10 years from the reconstructed flow of the SSR and NSR sub-basins, SRB (1400–2018). Multi-year sub-basin events highlighted in bold.

Cool Season				Warm Season			
Same years between sub-basins		SSR – Top 10 Years	NSR – Top 10 Years	Same years between sub-basins		SSR – Top 10 Years	NSR – Top 10 Years
Period	Year	1500	1697	Period	Year	1865	1889
1400s	1435, 1437, 1494	1492	1896	**1400s**	1437, **1474**, **1475**, 1489	1870	1919
1700s	1706, 1718, 1721	1485	1879			1435	1961
1900s	1941	1489	1423	**1500s**	**1503**, **1504**, 1556	1863	2010
2000s	2002	1573	1441	**1700s**	1706, 1721	1872	1484
		1988	1695	**1800s**	**1869**, **1870**	1479	1556
		1508	2002	**1900s**	1921, 1937, 1987	1489	1794
		1484	1895	**2000s**	2010	1846	1706
		1910	1475			1492	1987
		1556	1719			1437	1564

significant ($p < 0.05$) components of variability are found at interannual (2-6 year), inter-decadal (7–11 years) and multi-decadal time scales (20–30 years). Statistically significant ($p < 0.05$) inter-annual variability is evident throughout the wavelet power spectrum for all reconstructions.

Discussion and conclusions

The objective of this research was to provide water management agencies in the Canadian Prairie Provinces with robust palaeohydrological reconstructions of streamflow for the assessment of water delivery, allocation, storage, and treatment infrastructure and protocols under extreme hydroclimatic conditions. Many palaeohydrological studies throughout western Canada and North America (Watson and Luckman 2006; Axelson, Sauchyn, and Barichivich 2009; Starheim, Smith, and Prowse 2013; St. George 2014; Coulthard and Smith 2016; Crawford, Griffin, and Kipfmueller 2015; Coulthard, Smith, and Meko 2016; Dannenberg and Wise 2016; ; Sauchyn and Ilich 2017; Howard, Stahle, and Feng 2019; Lopez et al. 2019; ; Torbenson 2019; Welsh,

Table 5. Same years of low flow (defined by the 25th percentile) between sub-basins and the top 10 years from the reconstructed flow of the SSR and NSR sub-basins, SRB (1400–2018). Multi-year sub-basin events highlighted in bold.

Cool Season				Warm Season			
Same years between sub-basins		SSR – Top Years	NSR – Top Years	Same years between sub-basins		SSR – Top Years	NSR – Top Years
Period	Year	1500	1697	Period	Year	1865	1889
1400s	1428, 1433, **1435**, **1436**, **1437**, 1447, 1473, 1478, **1488**, **1489**, 1494	1492, 1485, 1489, 1573	1896, 1879, 1423, 1441	1400s	1402, 1408, 1437, **1446**, **1447**, 1474, 1475, 1479, **1489**, **1490**, 1498	1870, 1435, 1863, 1872	1919, 1961, 2010, 1484
1500s	1557, 1559, 1563, **1568**, **1569**, 1579	1988, 1508	1695, 2002	1500s	**1503**, **1504**, 1513, 1533, **1556**, **1557**, 1558, 1563, 1564, **1568**, **1569**	1479, 1489, 1846, 1492, 1437	1556, 1794, 1706, 1987, 1564
1600s	1624, 1664, 1695	1484	1895	1600s	1630, 1634, 1639, 1657, 1664, 1682, 1696		
1700s	1706, 1707, 1710, **1717**, **1718**, 1721, 1744, 1760	1910, 1556	1475, 1719	1700s	1706, **1720**, **1721**, 1759, 1773, 1794		
1800s	1859, 1864, 1870, 1883			1800s	1815, 1852, 1860, **1862**, **1863**, **1864**, **1865**, **1869**, **1870**		
1900s	**1919**, **1920**, 1937, 1939, 1941, 1945, 1964, 1984, 1995			1900s	1919, **1921**, **1922**, **1936**, **1937**, **1939**, **1940**, 1979, **1983**, **1984**, **1985**, 1987, 1992		
2000s	2002			2000s	2001, 2010		

Table 6. Same years of high flow (defined by the 75th percentile) between the sub-basins and the top 10 years from the reconstructed flow of the SSR and NSR sub-basins, SRB (1400–2018). Multi-year sub-basin events highlighted in bold.

Cool Season				Warm Season			
Same years between sub-basins		SSR – Top Years	NSR – Top Years	Same years between sub-basins		SSR – Top Years	NSR – Top Years
Period	Year	1669	1415	Period	Year	1839	1908
1400s	1409, 1417, 1444, 1450	1417, 1828	1901, 1788	1400s	1414, 1416, **1461**, **1462**	1405, 2013	1881, 1509
1500s	1511, 1520, **1531**, **1532**, 1550, 1552, **1589**, **1590**, 1592, **1598**, **1599**	1423, 1673, 1713, 1881	1751, 1681, 1516, 1974	1500s	1520, **1525**, **1526**, **1529**, **1530**, **1531**, **1537**, **1538**, **1539**, 1542, 1545, **1549**, **1550**, **1551**, 1599	1840, 1423, 1900, 1418, 2012	1598, 1901, 1549, 1897, 1508
1600s	1618, 1670, **1673**, **1674**, 1676	1419, 1672, 1952	1691, 1900, 1728	1600s	**1613**, **1614**, **1615**, 1617, 1621	1617, 1532	1529, 1788
1700s	1753, 1755, 1763, **1778**, **1779**, **1780**, 1782, **1788**, **1789**			1700s	1727, **1728**, 1753, 1754, **1778**, **1779**, **1780**, **1781**, **1782**		
1800s	1804, 1807, 1821, **1826**, **1827**, **1828**, **1829**, 1836, **1839**, **1840**, 1886			1800s	**1829**, **1830**, **1839**, **1840**, 1880, **1886**, **1887**, 1899		
1900s	**1901**, **1902**, **1903**, 1913, 1952, 1955, 1960, 1965			1900s	**1900**, **1901**, **1902**, **1903**, **1904**, **1908**, **1909**, 1914, **1916**, **1917**, 1948, 1951		
2000s	**2012**, **2013**, **2014**			2000s	2014		

Smith, and Coulthard 2019; Coulthard et al. 2021; Stahle et al. 2020; Wise 2021; Kerr, Andreichuk, and Sauchyn 2021) have shown that dendroclimatic extremes are outside the range of historical observations, and demonstrated that the hydroclimatic variability varies at decadal and multi-decadal time scales (Ault et al. 2013). Thus, these newly developed long-term seasonal perspectives of the regional hydroclimate are important for water management and climate change adaptation in the SRB.

In both seasons, tree-ring-reconstructed streamflow for the NSR and SSR recorded more severe and sustained droughts than during the modern instrumental era, demonstrating that persistent and widespread dryness occurred under natural conditions prior to anthropogenic forcing of regional and global climate. Ocean-atmospheric oscillations drive shifts in the strength of seasonal moisture persistence, and longer proxy records of the moisture regime, beyond the instrumental record, provide insights into the seasonal
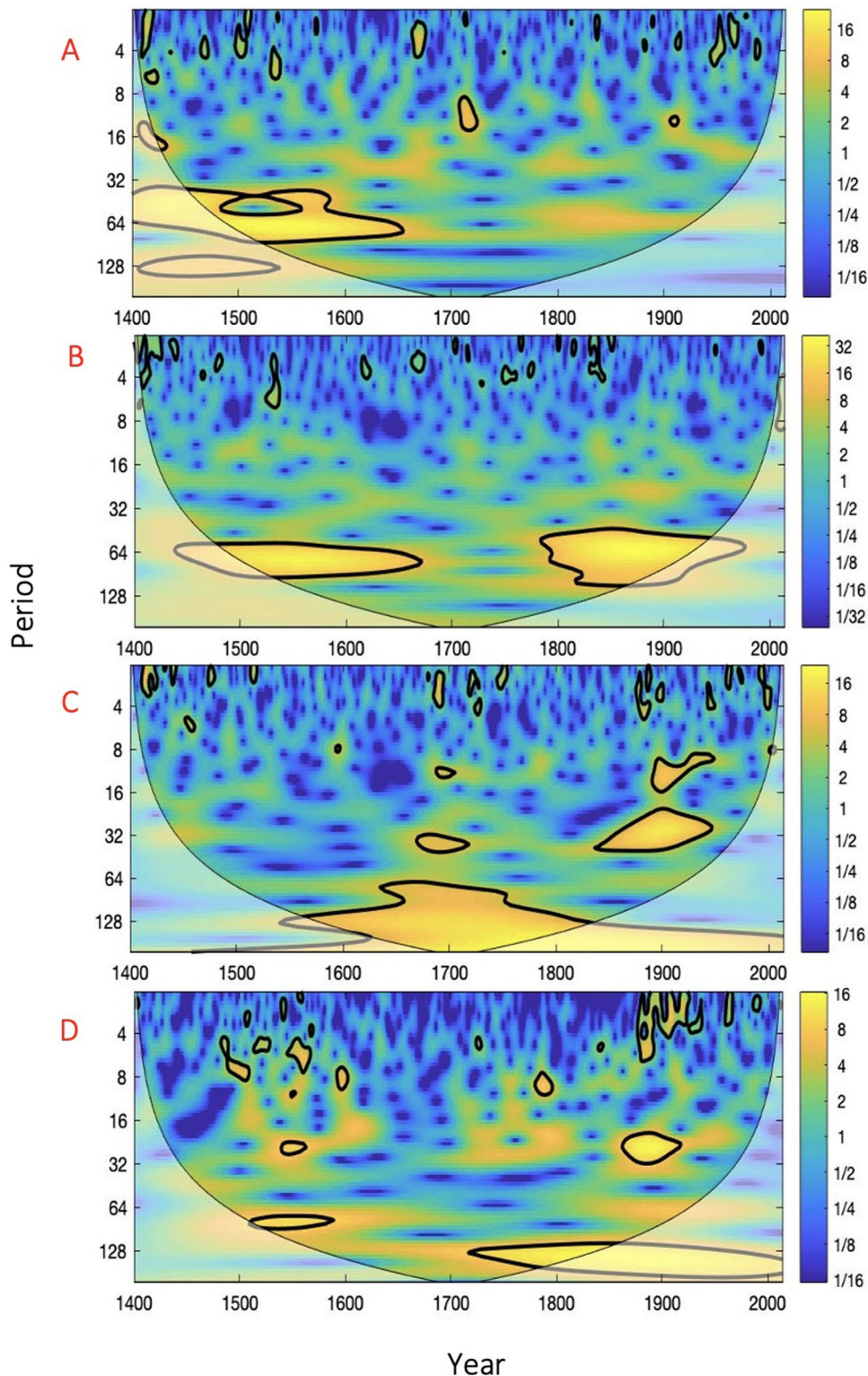
Figure 6. Continuous wavelet power spectrum for cool and warm season reconstructed streamflow (1400–2018) of the South Saskatchewan River (05AK001 at Highway 41) (A & B) and the North Saskatchewan River (05EF001 near Deer Creek) (C & D). The dark shade (highest power) and thick black contour lines indicate statistical significance at $p < 0.05$.

evolution of drought and excess moisture regimes throughout western Canada. Other comparisons of reconstructed streamflow, ENSO, and PDO (Woodhouse 1997; Stahle et al. 1998; D'Arrigo et al. 2001; MacDonald and Case 2005; Barrett, Jones, and Bigg 2018; Buckley et al. 2019) have similarly revealed higher cool season streamflow in the negative (cold) PDO phase and La Niña.

Our current study corresponds to previous reconstructions of streamflow in the NSR and SSR sub-basins (Case and MacDonald 2003; Axelson, Sauchyn, and Barichivich 2009; Sauchyn, Vanstone, and Perez-Valdivia 2011, Sauchyn, Luckman, and St-Jacques 2015a, Sauchyn et al. 2015), and any slight discrepancies in year-to-year differences are likely attributed to different sets of predictor tree-ring chronologies, and to our much larger and more recent (updated to 2018) network of moisture limited (based on the climate correlations of the predictors) chronologies from within and adjacent to both sub-basins, and for multiple species. The use of a large multi-species network for warm and cool seasonal reconstructions of streamflow within the SRB, shows their ability to capture negative anomalies. A key finding to this research is the ability to determine when both the NSR and SSR sub-basins were impacted by sustained droughts or excess moisture simultaneously.

From our tree-ring reconstructions of the seasonal flows of the NSR and SSR, we were able to determine: the seasonal hydroclimatic natural variability and trends (1400–2018); the spatial and temporal relationships for the two sub-basins in terms of the frequency and magnitude of flows; the quantified relationship between warm and cool seasonal anomalies of wet and dry periods throughout the NSR and SSR sub-basins; and the relationships between hydroclimate-related variables and the probable long-term influence of low- to high- frequency climate oscillations on that variability. For the cool season, there were 8, 43, and 51 similar years between the sub-basins defined by the 10th, 25th, and 75th percentiles, while for the warm season, there were 15, 60, and 54 similar years. The most sustained wet periods throughout the entire time series for the SSR (warm) were the mid-1500s and SSR (cool) was the 1400s and mid-1500s, while for the NSR (warm) was during the late-1400s, early-1500s, and late-1800s, and the late-1700s for the NSR (cool). The longest and most severe hydrological droughts occurred during the 1450s and 1850s for the SSR (warm) and the 1450s for the SSR (cool), while during the 1700s for the NSR (warm), and early-1400s, 1700s and late-1800s for the NSR (cool).

Differences in the strengths of the reconstructions for the SRB are likely related to model uncertainty, as well as the availability of long length statistically significant moisture sensitive chronologies to downstream gauge locations. The tree-ring network used for this study includes trees with a diversity of hydroclimatic sensitivities related to species, geography, topography, soils and hydroclimatic dynamics throughout the study region, which has allowed us to develop a better understanding of the complex regional hydroclimate and streamflow response (Wettstein et al. 2011; St. George 2014; Martin et al. 2019; Wise 2021). The proxy-based reconstructions are plausible estimates of the past hydroclimate of the SRB and these records of hydroclimatic variability have important implications for the long-term viability of existing water management practices.

While it is clear that there are dry and wet periods that exist throughout the reconstructed time series, the years of extreme hydroclimatic events indicate that there are more similarities between basins in both seasons during wet periods, than dry. It is also clear that there are more multi-year/basin events during the warm season for hydrological drought and low flow years, compared to years where excess streamflow occurred throughout the basins. The more frequent hydrological drought and synchronous events in the warm season likely reflect the greater sensitivity of tree growth to summer versus spring weather conditions. This research highlights the occurrence of multi-year and multi-basin events, where low flow and hydrological droughts can have detrimental effects on municipal, agricultural, industrial, and economic activity within the sub-basins of the SRB.

Acknowledgements

Disclosure statement

Funding

References

Anis, R. H., Y. Andreichuk, S. A. Kerr, and D. J. Sauchyn. 2021. "Climate Change Risks to Water Security in Canada's Western Interior." Chap. 2 in *Hydrological Aspects of Climate Change*, edited by A. Pandey, S. Kumar, and A. Kumar. Singapore: Springer Transactions in Civil and Environmental Engineering, pp. 25–61. doi: 10.1007/978-981-16-0394-5

Asong, Z. E., H. S. Wheater, B. Bonsal, S. Razavi, and S. Kurkute. 2018. "Historical Drought Patterns over Canada and Their Teleconnections with Large-Scale Climate

Signals." *Hydrology and Earth System Sciences* 22 (6): 3105–3124. doi:10.5194/hess-22-3105-2018.

Ault, T. R., J. E. Cole, J. T. Overpeck, G. T. Pederson, S. St. George, B. Otto-Bliesner, C. A. Woodhouse, and C. Deser. 2013. "The Continuum of Hydroclimate Variability in Western North America during the Last Millennium." *Journal of Climate* 26 (16): 5863–5878. doi: 10.1175/JCLI-D-11-00732.1.

Axelson, J. N., D. J. Sauchyn, and J. Barichivich. 2009. "New Reconstructions of Streamflow Variability in the South Saskatchewan River Basin from a Network of Tree Ring Chronologies, Alberta, Canada." *Water Resources Research* 45 (9): W09422. doi:10.1029/2008WR007639.

Barrett, H. G., J. M. Jones, and G. R. Bigg. 2018. "Reconstructing El Nino Southern Oscillation Using Data from Ships' Logbooks, 1815-1854. Part II: Comparisons with Existing ENSO Reconstructions and Implications for Reconstructing ENSO Diversity." *Climate Dynamics* 50 (9-10): 3131–3152. doi:10.1007/s00382-017-3797-4.

Bonsal, B. R., D. L. Peters, F. Seglenieks, A. Rivera, and A. Berg. 2019. "Changes in Freshwater Availability Across Canada." Chapter 6 in *Canada's Changing Climate Report*, edited by E. Bush and D. S. Lemmen. Ottawa, Ontario: Government of Canada, p. 261–342.

Bonsal, B. R., A. Shabbar, and K. Higuchi. 2001. "Impacts of Low Frequency Variability Modes on Canadian Winter Temperature." *International Journal of Climatology* 21 (1): 95–108. doi:10.1002/joc.590.

Bonsal, B. R., and A. Shabbar. 2008. "Impacts of Large-Scale Circulation Variability on Low Streamflows over Canada: A Review." *Canadian Water Resources Journal* 33 (2): 137–154. doi:10.4296/cwrj3302137.

Bonsal, B., and A. Shabbar. 2011. "Large-scale Climate Oscillations Influencing Canada,1900-2008." *Canadian Biodiversity: Ecosystem Status and Trends 2010*, Technical Thematic Report No. 4. Canadian Councils of Resource Ministers, Ottawa, ON. iii + 15 pp.

Buckley, B. M., C. C. Ummenhofer, R. D. D'Arrigo, K. G. Hansen, L. H. Truong, C. N. Le, and D. K. Stahle. 2019. "Interdecadal Pacifical Oscillation Reconstructed from trans-Pacific Tree Rings: 1350-2004 CE." *Climate Dynamics* 53 (5-6): 3181–3196. doi:10.1007/s00382-019-04694-4.

Case, R. A., and G. M. MacDonald. 2003. "Tree Ring Reconstructions of Streamflow for Three Canadian Prairie Rivers." *JAWRA Journal of the American Water Resources Association* 39 (3): 703–716. doi:10.1111/j.1752-1688.2003.tb03686.x.

Comeau, L. E. L., A. I. Pietroniro, and M. N. Demuth. 2009. "Glacier Contribution to the North and South Saskatchewan Rivers." *Hydrological Processes* 23 (18): 2640–2653. doi:10.1002/hyp.7409.

Cook, E. R. 1985. "A Time Series Analysis Approach to Tree-Ring Standardization." PhD. Diss., University of Arizona, Tucson. 171 pp.

Cook, E. R., and L. A. Kairiukstis. 1990. *Methods of Dendrochronology: Applications in the Environmental Science.* Doredrecht: Kluwer Academic Publishers, 394 pp.

Cook, E. R., and N. Pederson. 2011. "Uncertainty, Emergence, and Statistics in Dendrochronology." in *Dendroclimatology: Progress and Prospects*, edited by M. K. Hughes, T. W. Swetnam, and H. F. Diaz, 77–112, vol. 11. Dordrecht: Springer.

Cook, E. R., K. Briffa, S. Hiyatov, and V. Mazepa. 1990. "Tree-Ring Standardization and Growth- Trend Estimation." in *Methods of Dendrochronology: Applications in the Environmental Sciences*, edited by E. R. Cook and L. A. Kairiukstis, 104–123. Dordrecht, Netherlands: Kluwer Academic.

Cook, E. R., D. M. Meko, D. W. Stahle, and M. K. Cleaveland. 1999. "Drought Reconstructions for the Continental United States." *Journal of Climate* 12: 1145–1162.

Coulthard, B. L., and D. J. Smith. 2016. "A 477-Year Dendrohydrological Assessment of Drought Severity for Tsable River, Vancouver Island, British Columbia, Canada." *Hydrological Processes* 30 (11): 1676–1690. doi: 10.1002/hyp.10726.

Coulthard, B. L., K. J. Anchukaitis, G. T. Pederson, E. Cook, J. Littell, and D. J. Smith. 2021. "Snowpack Signals in North American Tree Rings." *Environmental Research Letters* 16 (3): 034037. in press. doi:10.1088/1748-9326/abd5de.

Coulthard, B., D. J. Smith, and D. M. Meko. 2016. "Is Worst-Case Scenario Streamflow Drought Underestimated in British Columbia? A 332-Year Perspective for the South Coast, Derived from Tree-Rings." *Journal of Hydrology* 534: 205–218. doi:10.1016/j.jhydrol.2015.12.030.

Crawford, C. J., D. Griffin, and K. F. Kipfmueller. 2015. "Capturing Season-Specific Precipitation Signals in the Northern Rocky Mountains, USA, Using Earlywood and Latewood Tree Rings." *Journal of Geophysical Research: Biogeosciences* 120 (3): 428–440. doi:10.1002/2014JG002740.

Dannenberg, M. P., and E. K. Wise. 2016. "Seasonal Climate Signals from Multiple Tree Ring Metrics: A Case Study of Pinus Ponderosa in the Upper Columbia River Basin." *Journal of Geophysical Research: Biogeosciences* 121 (4): 1178–1189. doi:10.1002/2015JG003155.

D'Arrigo, R., R. Villalba, and G. Wiles. 2001. "Tree-Ring Estimates of Pacific Decadal Variability." *Climate Dynamics* 18 (3-4): 219–224. doi:10.1007/s003820100177.

Draper, N. R., and H. Smith. 1998. *Applied Regression Analysis.* New York: Wiley, 69 and 330–346.

Fritts, H. C. 1976. *Tree Rings and Climate.* New York: Academic Press Inc.

Ghil, M., M. Allen, R. Dettinger, M. D. Ide, K. Kondrashov, D. Mann, M. E. Robertson, et al. 2002. "Advanced Spectral Methods for Climatic Time Series." *Reviews of Geophysics* 40 (1): 3–1–3.41. pp. doi:10.1029/2000RG000092.

Gobena, A. K., and T. Y. Gan. 2006. "The Role of Pacific Climate on Low-Frequency Hydroclimatic Variability and Predictability in Southern Alberta." *Canada.*" *Journal of Hydrometeorology* 10: 1467–1478.

Government of Alberta. 2010. *Facts about Water in Alberta.* Edmonton, Canada: Government of Alberta, 68 pp.

Griffin, R. D., C. A. Woodhouse, D. M. Meko, D. W. Stahle, H. L. Faulstich, C. Carrillo, R. Touchan, C. L. Castro, and S. W. Leavitt. 2013. "North American Monsoon Precipitation Reconstructed from Tree Rings." *Geophysical Research Letters* 40 (5): 954–958. doi:10.1002/grl.50184.

Grinsted, A., J. C. Moore, and S. Jevrejeva. 2004. "Application of the Cross Wavelet Transform and Wavelet Coherence to Geophysical Time Series." *Nonlinear Processes in Geophysics* 11 (5/6): 561–566. doi: 10.5194/npg-11-561-2004.

Gurrapu, S., J. M. St. Jacques, D. J. Sauchyn, and K. H. Hodder. 2016. "The Influence of the PDO and ENSO on the Annual Flood Frequency of Southwestern Canadian Prairie Rivers." *JAWRA Journal of the American Water Resources Association* 52 (5): 1031–1045. doi:10.1111/1752-1688.12433.

Gurrapu, S., K. R. Hodder, D. J. Sauchyn, and J. M. St. Jacques. 2021. "Assessment of the Ability of the Standardized Precipitation Evaporation Index (SPEI) to Model Historical Streamflow in Watersheds of Western Canada." *Canadian Water Resources Journal / Revue canadienne des ressources hydriques* 46 (1–2): 52–72. doi:10.1080/07011784.2021.1896390.

Holmes, R. 1983. "Computer-Assisted Quality Control in Tree-Ring Dating and Measurement." *Tree Ring Bulletin* 44: 69–75.

Howard, I. M., D. W. Stahle, and S. Feng. 2019. "Separate Tree-Ring Reconstructions of Spring and Summer Moisture in the Northern and Southern Great Plains." *Climate Dynamics* 52 (9-10): 5877–5897. doi:10.1007/s00382-018-4485-8.

Hughes, M. K., Kelly, P. M. Pilcher, J. R. Lamarche, Jr., and V. C. 1982. *Climate from Tree Rings*. Cambridge, U.K.: Cambridge University Press.

Kerr, S. A., Y. Andreichuk, and D. Sauchyn. 2021. "Warm and Cool Season Reconstruction and Assessment of the Long-Term Hydroclimatic Variability of the Canadian Prairie Provinces through the Development of the Canadian Prairies Paleo Drought Atlas (CPPDA)." *International Journal of Climatology* 41 (6): 3539–3560. doi:10.1002/joc.7034.

Kienzle, S. W., M. W. Nemeth, J. M. Byrne, and R. J. MacDonald. 2012. "Simulating the Hydrological Impacts of Climate Change in the Upper North Saskatchewan River Basin, Alberta, Canada." *Journal of Hydrology* 412-413: 76–89. doi:10.1016/j.jhydrol.2011.01.058.

Kulshreshtha, S., C. Nagy, and A. Bogdan. 2012a. "Present and Future Water Demand in the North Saskatchewan River Basin." University of Saskatchewan, Saskatoon, Saskatchewan, Canada (Research Report).

Kulshreshtha, S., C. Nagy, and A. Bogdan. 2012b. "Present and Future Water Demand in the South Saskatchewan River Basin." University of Saskatchewan, Saskatoon, Saskatchewan, Canada (Research Report).

Lapp, S. L., J. M. St. Jacques, D. J. Sauchyn, and J. R. Vanstone. 2013. "Forcing of Hydroclimatic Variability in the Northwestern Great Plains since AD 1406." *Quaternary International* 310: 47–61. doi:10.1016/j.quaint.2012.09.011.

Lilliefors, H. W. 1967. "On the Kolmogrov-Smirnov Test for Normality with Mean and Variance Unknown." *Journal of the American Statistical Association* 62 (318): 399–402. doi:10.1080/01621459.1967.10482916.

Lopez, E. L., S. A. Kerr, D. J. Sauchyn, and M. C. Vanderwel. 2019. "Variation in Tree Growth Sensitivity to Moisture across a Water-Limited Forest Landscape." *Dendrochronologia* 54: 87–96. doi:10.1016/j.dendro.2019.02.005.

MacDonald, G. M., and R. A. Case. 2005. "Variations in the Pacific Decadal Oscillation over the past Millennium." *Geophysical Research Letters* 32 (8): 1–4. doi:10.1029/2005GL022478.

MacDonald, R. J., J. M. Byrne, S. Boon, and S. W. Kienzle. 2012. "Modelling the Potential Impacts of Climate Change on Snowpack in the North Saskatchewan River Watershed." *Water Resources Management* 26 (11): 3053–3076. doi:10.1007/s11269-012-0016-2.

Mann, M. E., and J. M. Lees. 1996. "Robust Estimation of Background Noise and Signal Detection in Climatic Time Series." *Climatic Change* 33 (3): 409–445. doi:10.1007/BF00142586.

Marshall, S. J., E. C. White, M. N. Demuth, T. Bolch, R. Wheate, B. Menounos, M. J. Beedle, and J. M. Shea. 2011. "Glacier Water Resources on the Eastern Slopes of the Canadian Rocky Mountains." *Canadian Water Resources Journal* 36 (2): 109–134. doi:10.4296/cwrj3602823.

Martin, J. T., G. T. Pederson, C. A. Woodhouse, E. Cook, R. McCabe, G. J. Wise, E. K. Erger, et al. 2019. "1200 Years of Upper Missouri River Streamflow Reconstructed from Tree Rings." *Quaternary Science Reviews* 224: 105971–105915. doi:10.1016/j.quascirev.2019.105971.

McKenney, D. W., M. F. Hutchinson, P. Papadopol, K. Lawrence, J. Pedlar, K. Campbell, W. Milewska, R. F. Hopkinson, D. Price, and T. Owen. 2011. "Customized Spatial Climate Models for North America." *Bulletin of the American Meteorological Society* 92 (12): 1611–1622. doi:10.1175/2011BAMS3132.1.

Meko, D. M., and C. A. Woodhouse. 2011. "Application of Streamflow Reconstruction to Water Resources Management." in *Dendroclimatology: Progress and Prospects*, edited by M. K. Hughes, T. W. Swetnam, and H. F. Diaz, 231–261. New York: Springer.

Meko, D. M., and C. H. Baisan. 2001. "Pilot Study of Latewood Width of Conifers as an Indicator of Variability of Summer Rainfall in the North American Monsoon Region." *International Journal of Climatology* 21 (6): 697–708. doi:10.1002/joc.646.

Meko, D. M., C. A. Woodhouse, and K. Morino. 2012. "Dendrochronology and Links to Streamflow." *Journal of Hydrology* 412–413: 200–209. doi:10.1016/j.jhydrol.2010.11.041.

Mood, B. J., B. Coulthard, and D. J. Smith. 2020. "Three Hundred Years of Snowpack Variability in Southwestern British Columbia Reconstructed from Tree-Rings." *Hydrological Processes* 34 (25): 5123–5133. doi:10.1002/hyp.13933.

Mote, P. W., S. Li, D. P. Lettenmaier, M. Xiao, and R. Engel. 2018. "Dramatic Declines in Snowpack in the Western US." *Npj Climate and Atmospheric Science* 1 (1): 6. doi:10.1038/s41612-018-0012-1.

North Saskatchewan Watershed Alliance. 2007. *Current and Future Water Use in the North Saskatchewan River Basin*. Edmonton: NSWA, 30 pp.

Ostrom, C. W. 1990. "Time Series Analysis: Regression Techniques." *Quantitative Applications in the Social Sciences* (07-009), 2nd ed. Newbury Park, California: Sage.

Pomeroy, J. W., D. de Boer, and L. W. Martz. 2005. "Hydrology and Water Resources of Saskatchewan." in *Centre of Hydrology Report #1 Centre of Hydrology*, University of Saskatchewan, Saskatoon, Canada, 25 pp.

Regent Instruments Inc. 2019. in R. Guay (Ed.), *Windendro* (R. Gagnon, H. Morin Trans.). (b ed.). Canada: Regent Instruments Inc.

Rood, S. B., G. M. Samuelson, J. K. Weber, and K. A. Wywrot. 2005. "Twentieth-Century Decline in Streamflows from the Hydrographic Apex of North America." *Journal of Hydrology* 306 (1-4): 215–233. doi:10.1016/j.jhydrol.2004.09.010.

Sauchyn, D. J., B. H. Luckman, and J. M. St-Jacques. 2015a. "Long-Term Reliability of the Athabasca River (Alberta, Canada) as the Water Source for Oil Sands Mining." *Proceedings of the National Academy of Sciences* 112 (41): 12621–12626. doi:10.1073/pnas.1509726112.

Sauchyn, D. J., J. St. Jacques, E. Barrow, S. Lapp, C. Perez-Valdivia, and J. Vanstone. 2012. "Variability and Trend in Alberta Climate and Streamflow with a Focus on the North Saskatchewan River Basin." 2011-12 Final Report, Prairies RAC, 31 March 2012.

Sauchyn, D. J., J. Vanstone, J. M. St. Jacques, and R. Sauchyn. 2015. "Dendrohydrology in Canada's Western Interior and Applications to Water Resource Management." *Journal of Hydrology* 529: 548–558. doi:10.1016/j.jhydrol.2014.11.049.

Sauchyn, D., and N. Ilich. 2017. "Nine Hundred Years of Weekly Streamflows: Stochastic Downscaling of Ensemble Tree-Ring Reconstructions." *Water Resources Research* 53 (11): 9266–9283. doi:10.1002/2017WR021585.

Sauchyn, D., and S. Kulshreshtha. 2008. ""The Prairies." Chap. 7 in *From Impacts to Adaptation: Canada in a Changing Climate 2007*, edited by D. S. Lemmen, F. J. Warren, J. Lacroix and E. Bush. Ottawa, ON: Government of Canada, pp.275–328.

Sauchyn, D., J. Vanstone, and C. Perez-Valdivia. 2011. "Modes and Forcing of Hydroclimatic Variability in the Upper North Saskatchewan River Basin since 1063." *Canadian Water Resources Journal / Revue Canadienne Des Ressources Hydriques* 36 (3): 205–217. doi:10.4296/cwrj3603889.

Shabbar, A., and W. Skinner. 2004. "Summer Drought Patterns in Canada and the Relationship to Global Sea Surface Temperatures." *Journal of Climate* 17 (14): 2866–2880. doi:10.1175/1520-0442(2004)017<2866:SDPICA>2.0.CO;2.

St. George, S. 2014. "An Overview of Tree-Ring Width Records across the Northern Hemisphere." *Quaternary Science Reviews* 95: 132–150. doi:10.1016/j.quascirev.2014.04.029.

St. Jacques, J.-M., Y. Andreichuk, D. J. Sauchyn, and E. Barrow. 2018. "Projecting Canadian Prairie Runoff for 2041–2070 with North American Regional Climate Change Assessment Program (NARCCAP) Data." *JAWRA Journal of the American Water Resources Association* 54 (3): 660–675. doi:10.1111/1752-1688.12642.

St. Jacques, J.-M., S. L. Lapp, Y. Zhao, E. M. Barrow, and D. J. Sauchyn. 2014. "Twenty-First Century Central Rocky Mountain River Discharge Scenarios under Greenhouse Forcing." *Quaternary International* 310: 34–46. doi:10.1016/j.quaint.2012.06.023.

St. Jacques, J. M., D. J. Sauchyn, and Y. Zhao. 2010. "Northern Rocky Mountain Streamflow Records: Global Warming Trends, Human Impacts or Natural Variability?" *Geophysical Research Letters* 37 (6): 1–5. doi:10.1029/2009GL042045.

Stahle, D. W., E. R. Cook, D. J. Burnette, M. C. A. Torbenson, I. M. Howard, D. Griffin, J. V. Villanueva, et al. 2020. "Dynamics, Variability, and Change in Seasonal Precipitation Reconstructions for North America." *Journal of Climate* 33 (8): 3173–3195. doi:10.1175/JCLI-D-19-0270.1.

Stahle, D. W., M. K. Cleaveland, M. D. Therrell, D. A. Gay, R. D. D'Arrigo, P. J. Krusic, E. R. Cook, et al. 1998. "Experimental Dendroclimatic Reconstruction of the Southern Oscillation." *Bulletin of the American Meteorological Society* 79 (10): 2137–2152. doi:10.1175/1520-0477(1998)079<2137:EDROTS>2.0.CO;2.

Starheim, C. C. A., D. J. Smith, and T. D. Prowse. 2013. "Dendrohydroclimate Reconstructions of July-August Runoff for Two Nival-Regime Rivers in West Central British Columbia." *Hydrological Processes* 27 (3): 405–420. doi:10.1002/hyp.9257.

Stokes, M. A., and T. L. Smiley. 1968. *An Introduction to Tree-Ring Dating*. Tucson, AZ: University of Arizona Press.

Thompson, J. 2016. "An update on water allocation and use in the North Saskatchewan River Basin in Alberta." North Saskatchewan Watershed Alliance. https://www.nswa.ab.ca/wp-content/uploads/2017/09/Water-Use-Update-John-Thompson.pdf

Torbenson, M. C. A. 2019. "Cool and Warm Season Climate Signals in Tree Rings from North America." Theses and Dissertations, University of Arkansas, Fayetteville.

Torbenson, M. C. A., D. W. Stahle, J. Villanueva, E. R. Cook, and D. R. Griffin. 2016. "The Relationship between Earlywood and Latewood Tree-Growth across North America." *Tree-Ring Research* 72 (2): 53–66. doi:10.3959/1536-1098-72.02.53.

Watson, E., and B. H. Luckman. 2006. "Long Hydroclimate Records from Tree-Rings in Western Canada: Potential Problems and Prospects." *Canadian Water Resources Journal* 31 (4): 205–228. doi:10.4296/cwrj3104205.

Welsh, C., D. J. Smith, and B. Coulthard. 2019. "Tree-Ring Records Unveil Long-Term Influence of the Pacific Decadal Oscillation on Snowpack Dynamics in the Stikine River Basin, Northern British Columbia." *Hydrological Processes* 33 (5): 720–736. doi:10.1002/hyp.13357.

Wettstein, J. J., J. S. Littell, J. M. Wallace, and Z. Gedalof. 2011. "Coherent Region-, Species-, and Frequency-Dependent Local Climate Signals in Norther Hemisphere Tree Ring Widths." *Journal of Climate* 24 (23): 5998–6012. doi:10.1175/2011JCLI3822.1.

Whitfield, P. H., R. D. Moore, S. W. Fleming, and A. Zawadzki. 2010. "Pacific Decadal Oscillation and the Hydroclimatology of Western Canada—Review and Prospects." *Canadian Water Resources Journal* 35 (1): 1–28. doi:10.4296/cwrj3501001.

Wigley, T. M., K. R. Briffa, and P. D. Jones. 1984. "On the Average Value of Correlated Time Series, with Application in Dendroclimatology and Hydrometeorology." *Journal of Climate and Applied Meteorology* 23 (2): 201–213. doi:10.1175/1520-0450(1984)023<0201:OTAVOC>2.0.CO;2.

Wise, E. K. 2021. "Sub-Seasonal Tree-Ring Reconstructions for More Comprehensive Climate Records in U.S. West Coast Watersheds." *Geophysical Research Letters* 48 (2): 1–10. doi:10.1029/2020GL091598.

Woodhouse, C. A. 1997. "Tree-Ring Reconstructions of Circulation Indices." *Climate Research* 8: 117–127. doi:10.3354/cr008117.